Analytical 1D-calculation of a 1-turn Coil Parameters for the Magneto-Forming Technology

O. Mansouri[1*], O. Maloberti[1], D. Jouaffre[2], M. Hamzaoui[3], J. Derosiere[4], D. Haye[2], J. P. Leonard[5], P. Pelca[6]

[1] ESIEE Amiens, France ; [2] PFT Innovaltech, Saint-Quentin, France ; [3] LTI-UPJV, Saint Quentin, France ; [4] BASIS-EP, Saint-Quentin, France ; [5] INDUXIAL, Albert, France ; [6] CLAL France, Bornel, France
[*]Corresponding author. Email: mansouri@esiee-amiens.fr

Abstract

In this paper, we will present an analytical modelling of a one-turn coil dedicated to magnetic-pulse technologies. The goal is to be able to determine the main useful parameters of an inductor by calculating the magnetic vector potential "A" diffusion. The concerned parameters are electromagnetic (electromagnetic fields, magnetic flux and electric current densities), electrical (resistance and inductance, maximum field coefficient) and electromechanical (Lorentz force density and maximum force coefficient). The results obtained will then be compared to numerical computations performed onto some test cases. In order to get an approximate but robust analytical solution, it is proposed to assume an axial symmetry and to solve the problem in the harmonic working condition before studying the transient state.

Keywords

Magnetic pulse forming and welding, Analytical methods, Bessel functions

1 Introduction

Electromagnetic problems are usually divided into three categories: low, intermediate, and high frequency. At low frequencies, static conditions are assumed; at high frequencies, wave equations are used. Both of these regions have been studied extensively. However, in the intermediate frequency range, where diffusion equations are used, only a few problems have actually been solved. The induction problems concerning the magnetic pulse technology fall

into this intermediate frequency region (Jackson, 1999). The magneto-forming is a shaping process for conducting materials. It takes profit from the Lorentz force effects that the oscillating magnetic field produces on a metal in which eddy currents are induced. The stake is the evaluation of this force through the fields and currents.

This paper proposes an analytical method in order to calculate the electromagnetic fields and densities that are generated by the current pulse in the inductor used in the magneto-forming technology. Different geometries of inductors are used to generate electromagnetic pulses. In several applications the single turn coil is preferable to the multi-turn coil because it is more robust (Psyk et al., 2011) and (Wilson et al., 1965). Single turn coils are used in pulsed magnetic technologies for which both magneto-harmonic and transient magnetic analyses are required. We suggest studying one single turn coil example made of a conducting massive coil. Due to a cut within the toroïdal coil between the two terminals, it is rigorously a 3D component with no axial symmetry. Because this cut is very small, we would like to investigate the possibility to reduce this geometry into an equivalent 2D and then 1D axi-symmetrical model, giving with good approximation the solution. Since the coil is highly conducting and the source is varying very quickly in time (from 10 to 100 kHz), we suggest computing the model with time harmonics in order to analyse the eddy currents, skin effects and induced Lorentz forces.

In the following we will first derive the general 1D Partial Differential Equation (PDE) in cylindrical coordinates, then solve the problem in the harmonic working condition, finally give the results onto the main electromagnetic fields, densities, and electrical and electromechanical parameters, before concluding.

2 Theory

The equations for the vector potential $\vec{A}$ can be derived from the Maxwell's equations:

$$\vec{\nabla} \wedge \vec{H} = \vec{j} + \frac{\partial \vec{D}}{\partial t}$$
(1)

$$\vec{\nabla} \wedge \vec{E} = -\frac{\partial \vec{B}}{\partial t}$$
(2)

$$\vec{\nabla} \cdot \vec{B} = 0$$
(3)

$$\vec{\nabla} \cdot \vec{E} = \frac{\rho}{\varepsilon}$$
(4)

The medium is assumed to be linear, isotropic and homogeneous; the following relationships between $\vec{D}$ and $\vec{E}$, and $\vec{B}$ and $\vec{H}$ hold: $\vec{B} = \mu \vec{H}$ (5), $\vec{D} = \varepsilon \vec{E}$ (6); μ and ε are respectively the absolute magnetic permeability and dielectric permittivity. The current density $\vec{j}$ can be expressed in terms of the Ohm's law: $\vec{j} = \sigma \vec{E}$ (7); where σ is the electric conductivity.

Eq. 6 and **Eq. 7** may be substituted into **Eq. 1** to obtain the curl of $\vec{H}$ in terms of $\vec{E}$:

$$\vec{\nabla} \wedge \vec{H} = \sigma\vec{E} + \frac{\partial \varepsilon\vec{E}}{\partial t}$$

(8)

The term $\sigma\vec{E}$ is much greater than $\partial(\varepsilon\vec{E})/\partial t$, so the latter may be neglected for frequencies below about ten megacycles per second (Dodd et al., 1968) and (Dodd, 1967). The magnetic induction field $\vec{B}$ may be expressed as the curl of a magnetic vector potential $\vec{A}_i$, **Eq. 9** replacing **Eq. 9** in **Eq. 2** and **Eq. 7** give **Eq. 10** and **Eq. 11.**

$$\vec{B} = \vec{\nabla} \wedge \vec{A}_i$$

(9)

$$\vec{\nabla} \wedge \vec{E} = -\frac{\partial}{\partial t}\vec{\nabla} \wedge \vec{A}_i = -\vec{\nabla} \wedge \frac{\partial \vec{A}_i}{\partial t}$$

(10)

$$\vec{j} = \sigma\vec{E} = -\sigma\frac{\vec{A}_i}{\partial t} - \sigma\vec{\nabla}V$$

(11)

where V *is* an electric scalar potential. The coil may be driven by a voltage generator with an applied voltage V. The total electric field $\vec{E}$ is thus the sum of the source field $\vec{E}_s = -\vec{\nabla}V$ and the induced field $\vec{E}_i = -\partial_t\vec{A}_i$. In the following, we investigate the possibility to look after a total magnetic potential $\vec{A}$ responsible for the total electric field $\vec{E}$ and the total electric current density $\vec{j}$ such that:

$$\vec{E} = -\frac{\partial\vec{A}}{\partial t}, \ \vec{j} = -\sigma\frac{\partial\vec{A}}{\partial t} \text{ and } \vec{B} = \vec{\nabla} \wedge \vec{A}$$

(12)

By using the Coulomb gauge $\vec{\nabla}.\vec{A} = 0$, **Eq. 12**, **Eq. 9** and **Eq. 5** into **Eq. 1**, we obtain:

$$\Delta\vec{A} - \mu\sigma\frac{\partial\vec{A}}{\partial t} = 0$$

(13)
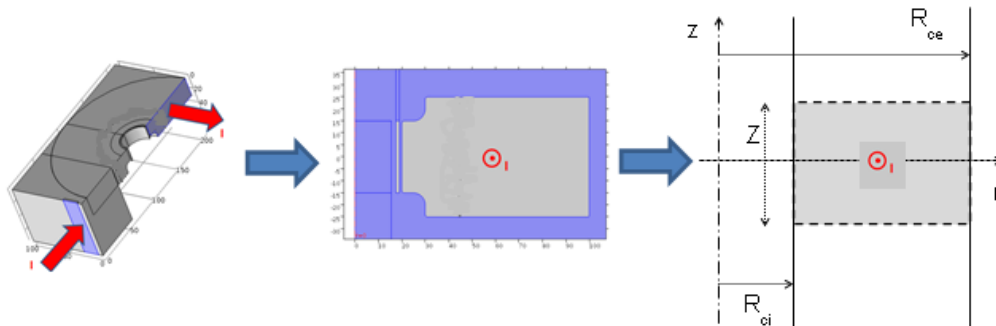
Figure 1: *Geometry of the 3D geometry and its 2D reduced model*

Fig.1 shows the inductor in 3, 2 and 1 dimensions respectively. The present analytical model is made on the basis of a 1D scheme. In 1D axial symmetric model only the (orthoradial) components A_Φ and j_Φ are present in the magnetic vector potential $\vec{A}$ and in the current density $\vec{j}$. Then, we obtain the homogeneous Partial Differential Equation (PDE) **Eq. 14** of the inductor in cylindrical coordinates (r, ϕ, z) while neglecting both the z and ϕ dependences.

$$\frac{\partial^2 A_\phi}{\partial r^2} + \frac{1}{r}\frac{\partial A_\phi}{\partial r} - \frac{A_\phi}{r^2} - \mu\sigma\frac{\partial A_\phi}{\partial t} = 0 \tag{14}$$

3 Harmonic Model

Assuming that both the voltage V and the total current I are sinusoidal functions of time, $V \equiv Ve^{i(\omega t+\varphi)}$ and $I \equiv Ie^{i\omega t}$. Then the vector potential is likewise a sinusoidal function of time, $A_\phi \equiv A_\phi e^{i\omega t}$, with A_ϕ a complex magnitude. **Eq. 14** is then written as follows:

$$\frac{\partial^2 A_\phi}{\partial r^2} + \frac{1}{r}\frac{\partial A_\phi}{\partial r} - \frac{A_\phi}{r^2} - i\omega\mu\sigma A_\phi = 0 \tag{15}$$

3.1 General Solution of the Homogeneous PDE

By using the global form of vector potential A, we consider that the total current density is included in the vector potential equation. For this, The 1D PDE and its solution in the harmonic working condition are given in **Eq. 16** and **Eq. 17.** (μ is the magnetic permeability of the coil, σ is the electrical conductivity of the coil, ω is the angle velocity of the current, $\alpha^2 = \mu\sigma\omega$. **Eq. 16**, is called the modified Bessel equation, for which the solution is given by **Eq. 17** (Andrew Gray et al., 1985) and (Figueiredo Jardim et al., 1989).

$$r^2\frac{\partial^2 A_\phi}{\partial r^2} + r\frac{\partial A_\phi}{\partial r} - (1 + ir^2\alpha^2)A_\phi = 0 \tag{16}$$

$$A_\phi(r, \omega) = C_1 J_1(\alpha_1 r) - i * C_2 K_1(\alpha_2 r) \tag{17}$$

With $\alpha_1 = \alpha.r.e^{(\frac{3\pi}{4}i)}$ and $\alpha_2 = \alpha.r.e^{(\frac{\pi}{4}i)}$, and where J_1 is the Bessel function of order 1 and first kind, and K_1 is the modified Bessel function of order 1 and second kind. The constants C_1 and C_2 can be determined from the boundary conditions and constraints (see next section).

3.2 Complete Solution with Limit Conditions and Constraints

We now need a limit condition on the surface field, and a total current constraint, and we assume that the inductor has a finite equivalent length Z_2 along the z axis (even if no z dependence is considered, see § 3.3).

$$I = \int_{R_{ci}}^{R_{ce}} \int_{-Z_2/2}^{+Z_2/2} j \, dr \, dz = -\sigma Z_2 i\omega \int_{R_{ci}}^{R_{ce}} A_{\emptyset}(r,\omega) dr \tag{18}$$

$$I = \oint H dl = H_z(R_{ci},\omega) Z_2 = \frac{B_z(R_{ci},\omega) Z_2}{\mu_0} = \frac{Z_2}{\mu_0} \left(\frac{A_{\emptyset}(R_{ci},\omega)}{R_{ci}} + \partial_r A_{\emptyset}(R_{ci},\omega) \right) \tag{19}$$

After some mathematical operations, we get:

$$C_1 = \frac{C_{12} K_0(\alpha_2 R_{ci}) - C_{22}(K_0(\alpha_2 R_{ce}) - K_0(\alpha_2 R_{ci}))}{K_0(\alpha_2 R_{ci})(J_0(\alpha_1 R_{ce}) - J_0(\alpha_1 R_{ci})) - J_0(\alpha_1 R_{ci})(K_0(\alpha_2 R_{ce}) - K_0(\alpha_2 R_{ci}))} \tag{20}$$

$$C_2 = \frac{C_{22}(J_0(\alpha_1 R_{ce}) - J_0(\alpha_1 R_{ci})) - C_{12} J_0(\alpha_1 R_{ci})}{K_0(\alpha_2 R_{ci})(J_0(\alpha_1 R_{ce}) - J_0(\alpha_1 R_{ci})) - J_0(\alpha_1 R_{ci})(K_0(\alpha_2 R_{ce}) - K_0(\alpha_2 R_{ci}))} \tag{21}$$

where:

$$C_{12} = \frac{I \alpha_2}{\sigma Z_2 \omega} \tag{22}$$

$$C_{22} = -i \frac{I \mu_0}{Z_2 \alpha_2} \tag{23}$$

3.3 How to Include the Z Dimension

The analytical model is calculated in one dimension for which the total length Z of the inductor should tend to the infinite. To qualify this modeling, we have compared the results to 2D numerical results obtained with the Finite Element method. The discrepancy between analytical and numerical results is mainly due to the finite Z dependence of the actual electromagnetic fields and densities. In order to reduce this error, we must take the dimension « Z » into account. In the 2D numerical simulations, we can observe that the current density j is expanding along the direction z with a longer equivalent length $Z_2=(Z+2\Delta Z)$, including the edges of equivalent length ΔZ at both sides (Fig. 2). As a conclusion, we propose to use Z_2 instead of Z inside the previous solution. The absolute and relative difference $2\Delta Z$ between Z_2 and Z can be expressed and estimated as a function of R_{ci} and $Z : \Delta Z = (Z_2-Z)/2 = f(Z,Rci)$ (24). The first analysis consists in adjusting the value of ΔZ for a fixed radius R_{ci} and various coil length Z, in order to fit the 2D numerical data. We observe that ΔZ depends only very slightly on the length Z, but the relative error $\Delta Z/Z$ is rapidly decreasing when the length is increasing, rendering the 1D assumption more relevant (Fig. 2). Next analysis might consider the dependence of the relative error $\Delta Z/Z$ on the radius Rci; which should be easier to interpret thanks to an analytical 2D model.
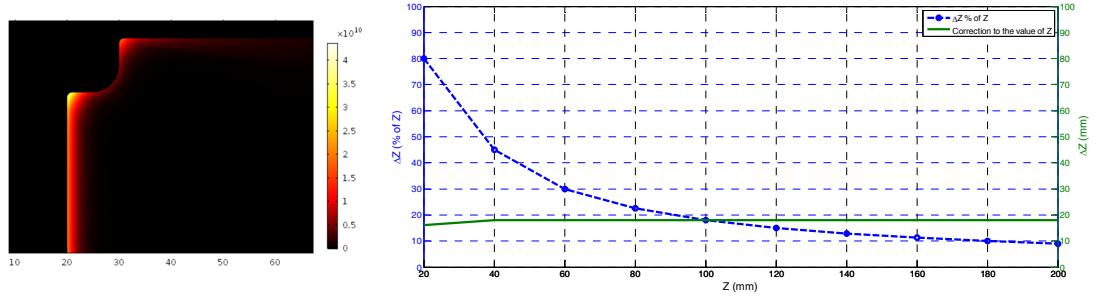
Figure 2: *Numerical computation of the current density distribution and variation of the ΔZ correction factor according to the length Z of inductor.*

3.4 How to Compute Electrical and Electromechanical Parameters

The magnetic vector potential solution $\vec{A}$ in Eq. 17 can be used to compute the whole electromagnetic fields $\vec{B}$, $\vec{H}$, $\vec{E}$ and $\vec{J}$ thanks to Eq. 12, Eq. 5 and Eq. 7. As a consequence, it becomes finally possible do deduce global quantities such as the Joule losses Pj=∭(j2/(2σ))d3x, the equivalent coil resistance R (Eq. 25), the stored magnetic energy Wm-Wm0=∭(jA/2)d3x, the equivalent coil inductance L (Eq. 26), the maximum field coefficient Kb (Eq. 27) and the maximum force density coefficient Kf (Eq. 28).

$$P_j = \iiint_{coil} \frac{1}{2}\sigma(\omega A)^2 r dr d\emptyset dz \ and \ R = \frac{2P_j}{I^2} \tag{25}$$

$$W_m = W_{m0} + \iiint_{coil} \frac{1}{2}\sigma\omega A^2 r dr d\emptyset dz \ and \ L = \frac{2W_m}{I^2} \tag{26}$$

$$B_{max} = max\{|\vec{B}\cdot\vec{u_z}|\} \ and \ K_b = \frac{B_{max}}{(I/(Z*(R_{ce}-R_{ci})))} \tag{27}$$

$$f_{max} = max\{|\vec{f}\cdot\vec{u_r}|\} \ and \ K_f = \frac{f_{max}}{\omega(I/(Z*(R_{ce}-R_{ci})))^2} \tag{28}$$

4 Simulation and Experimental Results

The geometrical parameters of the inductor are given in the Appendix; the coil length is: *Z=20…200 mm*; the current peak is: *I=825(Z[mm]/30) kA (I/(Z*(R$_{ce}$-R$_{ci}$))* stays constant, the reference current being 825 kA when *Z=30 mm*); the frequency is: *F = 20 kHz*.
In the following, we will analyze the results on *j*, *B* and *f* obtained as follow:

$$\vec{j} = j\vec{u_\varphi} = -\sigma\omega A\vec{u_\varphi} \tag{29}$$

$$\vec{B} = B\vec{u_z} = \left(\frac{A}{r} + \frac{\partial A}{\partial r}\right)\vec{u_z} \tag{30}$$

$$\vec{f} = f\vec{u_r} = real(j.B^*)\vec{u_r} \tag{31}$$

4.1 Electromagnetic Fields and Densities

Fig. 2, **Fig. 3** and **Fig. 4** show the results obtained for the magnitude of the current density |j|, the flux density |B| and the Lorentz force density |f| respectively (complex modules).
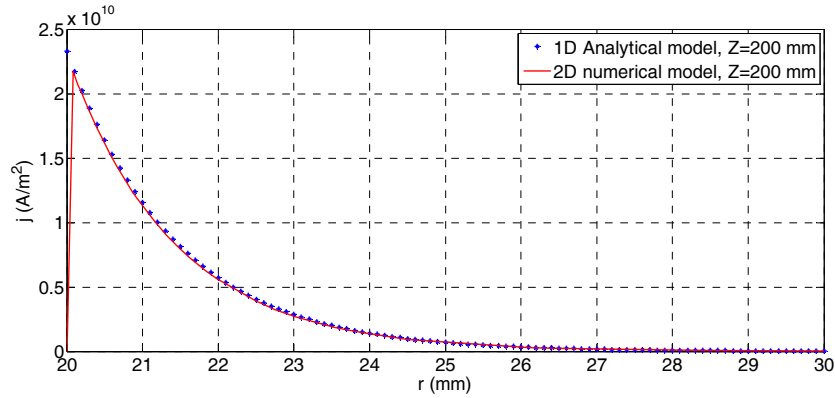

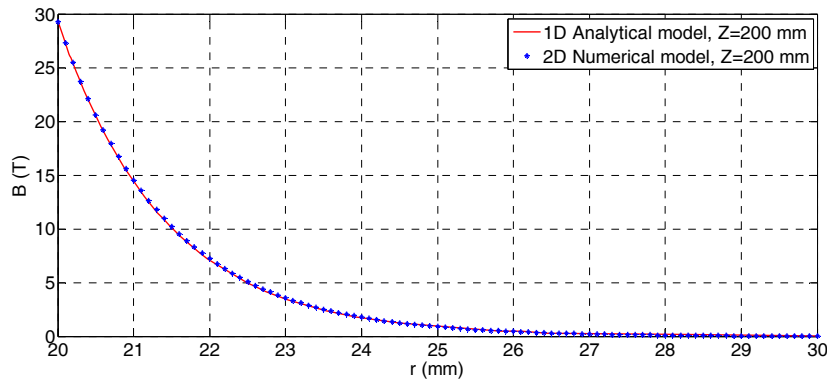*Figure 3*: *Current density distribution inside the coil (Z = 200 mm)*

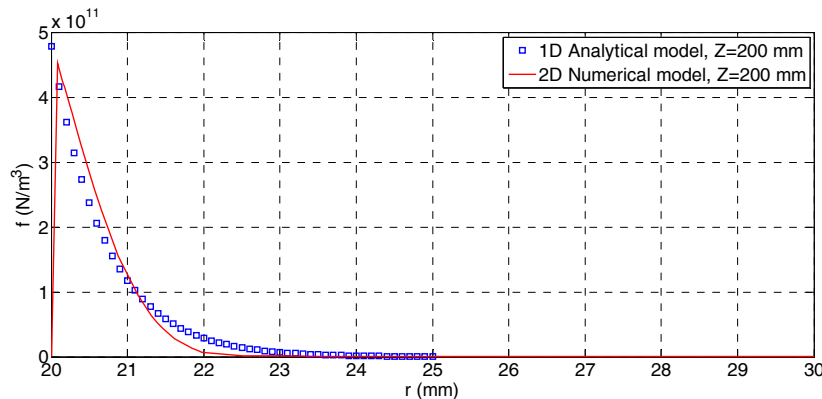*Figure 4*: *Magnetic flux density distribution inside the coil (Z = 200 mm)*

Figure 5: *Lorentz force density distribution inside the coil (Z = 200mm)*

Fig. 3, Fig. 4 and Fig. 5 show an interesting agreement between numerical and analytical calculations for the main tendency due to the skin effect. The discrepancy is due to the dependence on z coordinate but this last can however be reduced thanks to the ΔZ

correction factor (see Fig. 2 and Fig. 6). Either any disparity between the two methods or any deterministic relationship between ΔZ, R_{ci} and Z can be improved and found by a 2D resolution.
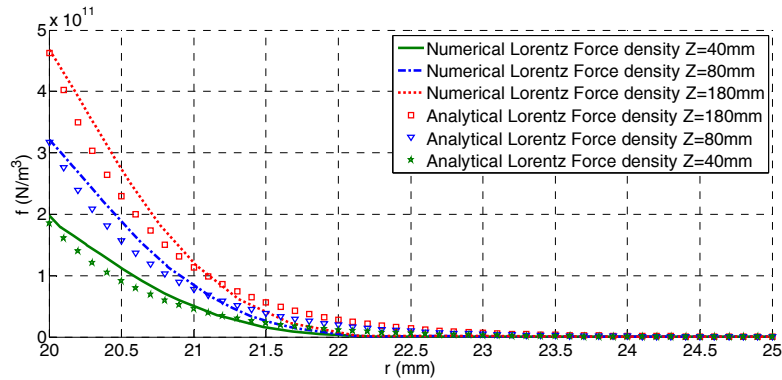

Figure 6: *Lorentz force density distribution inside the coil (Z = 40, 80 and 200 mm)*

Finally, it is possible to go further in the modelling technique by either considering:

1) the reduced potential $\vec{A_i}$ and the source field inside **Eq. 13** to **Eq. 16**,
2) the transient effect by solving the time dependent **Eq. 14**,
3) the z dependence by solving the 2D PDE coming from **Eq. 13**,
4) any second or third region to model a field shaper or a tube to deform.

4.2 Electrical and Electromechanical Parameters

In this section Fig. 7 and Fig. 8 show the results obtained for the electrical (equivalent coil resistance R and inductance L) and electromechanical (maximum field coefficient K_b and maximum force density coefficient K_f) parameters respectively (see **Eq. 25**, **Eq. 26**, **Eq. 27** and **Eq. 28**).
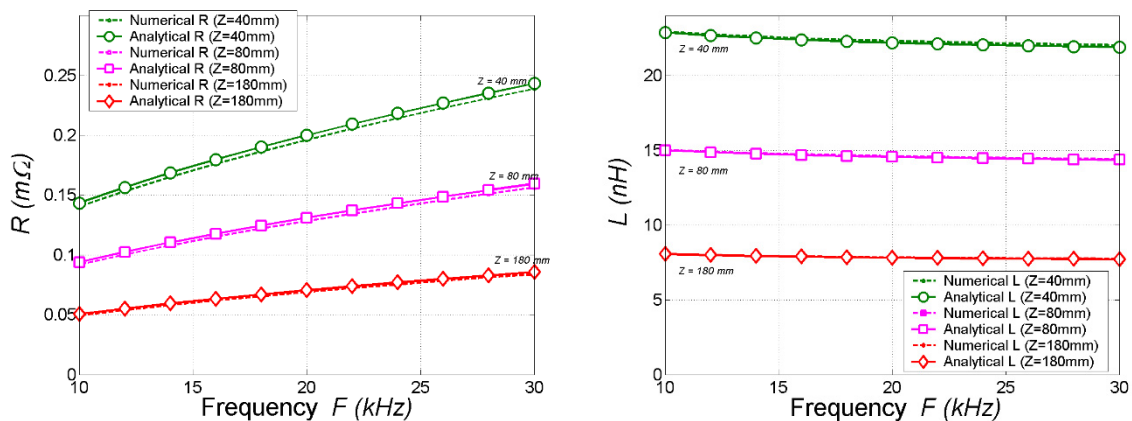
Figure 7: *The equivalent coil resistance and coil inductance defined by **Eq. 25** and **Eq. 26** as a function of the frequency F (Z = 40, 80 and 180 mm).*

As expected, we can see on figures Fig. 7 that the resistance is increasing while increasing the frequency (skin effect resistance) and decreasing while increasing the coil length or section. For similar reasons, the inductance is decreasing while increasing the frequency (skin effect inductance) and also decreasing while increasing the coil length or section.
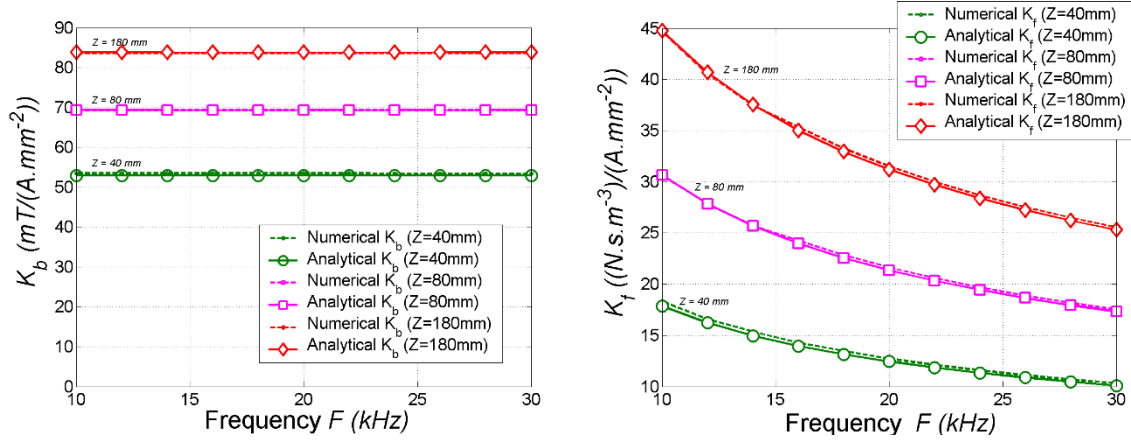
Figure 8: *The maximum field coefficient and the maximum force density coefficient defined by Eq. 27 and Eq. 28 as a function of the frequency F (Z = 40, 80 and 180 mm).*

In the same time, we can see on figures Fig. 8 that the maximum field coefficient stays constant whatever the frequency is (no skin effect dependent) and that this coefficient is increasing while increasing the coil length but with a limit around 101 mT/(A.mm^{-2}) which corresponds to the perfect infinite coil. Finally the maximum force density coefficient is decreasing while increasing the frequency and increasing while increasing the coil length but still with a limit around 65 (N.s.m^{-3})/((A.mm^{-2})^2).

The figures Fig. 7 and Fig. 8 permit to check that the 1D model proposed is also able to compute the main electrical and electromechanical parameters as a function of the frequency F and the coil length Z. All the main parameters are correctly computed but unfortunately, an unknown initial stored energy W_{m0} is necessary to get the correct inductance value. This might be due to the choice of the total magnetic vector potential instead of the reduced potential $\vec{A_i}$ inside **Eq. 13** to **Eq. 16**.

5 Conclusion

Starting from the general 1D Partial Differential Equation (PDE) and using a series development in a space of well-chosen base functions, it is possible to get a simple analytical solution. This method might ease the couplings between electrical, electromagnetic and mechanical effects. This method will help for: 1) the magnetic pulse process simulation, 2) the inductor sizing and optimization, 3) the choice of optimal working conditions.

Acknowledgments

References

Jackson, J. D., 1999, Classical Electrodynamics, Third Edition, John Wiley & Sons, Inc.

Psyk, V., Risch, D., Kinsey, B. L., Tekkaya, A. E., Kleiner, M., 2011, Electromagnetic Forming – A review, Journal of Materials Technology 211 (2011) 787 – 829.

Wilson, M. N., Srivastava, K. D., 1965, Design of Efficient Flux Concentrators for Pulsed High Magnetic Fields, The Review of Scientific Instruments, Vol. 36, N° 8, August 1965,

Dodd, C. V. and Deeds, W. E., 1968, Analytical Solutions to Eddy-Current Probe-Coil Problems, J. Appl. Phys. 39, 2829,1968.

Dodd, C. V., 1967, A Solution to Electromagnetic Induction Problems, M. S. Thesis, University of Tennessee, Oak Ridge National Laboratory, 1967.

Andrew Gray, M.A., G. B. Mathews, M.A., 1985, a treatise on bessel functions and their applications to physics, Macmillan and co. and New York. 1985.

Figueiredo Jardim, R., Laks, B., 1989, Kelvin functions for determination of magnetic susceptibility in nonmagnetic metals, J. Appl. Phys. 65(12), 15 June 1989.

Appendix A   Geometrical and Physical Parameters

A.1   Parameters of the Coil Geometry

Name	Value	significance
R_{ci}	20 mm	Internal coil radius
R_{cii}	30 mm	Intermediate coil radius
R_{ce}	100 mm	External coil radius

Table 1: *Parameters of the coil geometry*

A.2   Parameters of the Materials

Name	Value	significance
μ_0	$4\pi.10^{-7}$ H.m^{-1}	Vacuum magnetic permeability
σ_c	10 % IACS*	Coil electrical conductivity
σ_{Cu}	5.8 e^7 S.m^{-1}	Copper electrical conductivity

Table 2: *Parameters of the materials (@20°C)*

*IACS: International Annealed Copper Standard (100 % IACS = σ_{Cu})